Eur. Phys. J. D **46**, 165–172 (2008)
DOI: 10.1140/epjd/e2007-00272-8

THE EUROPEAN PHYSICAL JOURNAL D

Generation of maximally entangled atom pairs in driven dissipative cavity QED systems

F. Casagrande[a] and A. Lulli[b]

Dipartimento di Fisica, Università degli Studi di Milano, Via Celoria 16, 20133 Milano, Italy

Received 27 March 2007 / Received in final form 10 July 2007
Published online 26 September 2007 –

Abstract. We investigate the entanglement of an open tripartite system where a cavity field mode in thermal equilibrium is off-resonantly coupled with two atoms that are simultaneously driven by a resonant coherent field. For moderately detuned atom-field coupling and strong atomic driving we show the generation, at given interaction times and for low enough cavity decay rates, of atomic Bell states and of Bell state superpositions relevant for quantum gates implementation. The system can oscillate between bi-separable and fully separable states. Also we describe the distribution of quantum correlations between the atom-atom and the two atom-field subsystems. In the dispersive coupling regime with strongly driven atoms we show the generation of nearly stationary Bell states which remain protected from cavity dissipation.

PACS. 42.50.Pq Cavity quantum electrodynamics; micromasers – 03.67.Mn Entanglement production, characterization, and manipulation

1 Introduction

Since the early years of quantum mechanics entanglement was recognized as one of the most peculiar and puzzling feature of the theory [1]. Much later the Bell theorem [2] and the related experiments, in particular by Aspect and coworkers [3], made this issue regain a central role [4]. More recently entanglement has become a basic resource in quantum information (QI) [5]. In particular, the entanglement properties of multipartite systems are the object of intense research [6], also in the case of systems composed by qubits and Continuous Variable (CV) subsystems [7].

To implement QI processes many physical systems have been proposed such as atom-photon systems, nuclear and electron spins, quantum dots, superconductive quantum interference devices [8]. Current technological efforts are devoted to realize experimental setups to better satisfy the requirements of robust representation of quantum information, easy realization of unitary transformations (quantum gates), fiducial preparation of the initial states, and precise measurement of the output results.

In this paper we focus our attention on Cavity Quantum Electrodynamics (CQED) systems, where atoms and photons interact inside a cavity in the microwave or in the optical domain [9–11]. Typically, the atoms excited to long-lived Rydberg levels are injected into the cavity either flying through it or being trapped inside; recent improvements allow to trap one or few atoms in a deterministic way [12]. Recent achievements include e.g. the demonstration of entangled states between two atoms [13,14], two photons [15], one atom and one photon [16], the teleportation of an atom-photon state [17] and of a quantum state from light onto matter [18]. In the framework of trapped ions parallel results have been recently achieved [19].

The interaction between an atom and a cavity mode field is ruled by the well-known Jaynes-Cummings (JC) model [20] for both resonant and off-resonant coupling. An additional coherent field that drives the cavity mode or the atom can be added to the atom-field interaction [21]. In particular, it has been shown that at resonance and in the strong driving regime the whole atom-field-driving coupling can simultaneously realize the JC and the "anti-JC" dynamics in CQED [22]. Most related works have focussed on either the resonant or the dispersive regimes of atom-cavity field coupling [23–25]. We note here that in the framework of trapped ions [9] the JC and "anti-JC" dynamics can be implemented in the interaction between the atomic transition and the vibrational modes of the ions system.

In this paper we investigate the dynamics of a CQED system composed by a pair of coherently driven two-level atoms coupled to a cavity mode also interacting with a thermal bath. We propose to solve the whole system dynamics by means of the Monte Carlo Wave Function (MCWF) approach [26] to fully investigate all regimes also in the presence of cavity and atomic decays. In fact, we can

[a] e-mail: federico.casagrande@mi.infn.it
[b] e-mail: alfredo.lulli@unimi.it

generalize early work as in [27] where the conditioned two-atoms dynamics was solved only in the strong-detuning and low-driving regimes under the condition of the cavity field always in the vacuum state. We remark that with current CQED technology it should be possible to implement our scheme in the case of atoms flying through the cavity [9]. In the case of atoms trapped inside the cavity, that is the better perspective for quantum computation, further improvements in the neutral atoms trapping technology [28] should allow to implement our scheme in the near future. An alternative approach to trapped neutral atoms may be that of using two ions trapped inside a high finesse optical cavity [29], where the interaction between the atoms is mediated by the cavity mode while the vibrational degrees are cooled to the ground state.

From our analysis two regimes emerge as quite promising for the generation of maximally entangled bi-atomic Bell states at given interaction times or even stationary: namely, the regimes of moderate or large atom-field detuning, in both cases under strong atom-field coupling and strong atomic driving conditions. In the first regime also Bell state superpositions can be generated such that one could implement with the atom pair a logic gate suggested [23] and demonstrated [30] with two trapped ions. Furthermore, the physical mechanism for atomic entanglement is in principle scalable for quantum information/computation purposes.

In Section 2 we introduce the system and the methods to investigate its dynamics. In Section 3 we describe the open system dynamics in the strong coupling regime of CQED, both on- and off-resonance and for different detuning and driving conditions. The effects of cavity and atomic dissipation are treated in Section 4. Conclusive remarks are reported in Section 5.

2 System dynamics description

We consider a pair of identical two-level Rydberg atoms whose relevant energy eigenstates are $|g\rangle_i$, $|e\rangle_i$ $(i = 1, 2)$. Both atoms interact simultaneously and for the same interaction time t with a cavity mode and an external coherent driving field at frequencies ω_c and ω_f, respectively. The system Hamiltonian can be written as $\hat{H}(t) = \hat{H}_0 + \hat{H}_1(t)$, where

$$\hat{H}_0 = \hbar\omega_c\hat{a}^\dagger\hat{a} + \frac{\hbar\omega_a}{2}\sum_{i=1}^{2}\hat{\sigma}_{z,i}$$

$$\hat{H}_1(t) = \hbar\sum_{i=1}^{2}[g(\hat{a}\hat{\sigma}_i^\dagger + \hat{a}^\dagger\hat{\sigma}_i) + \Omega(e^{i\omega_f t}\hat{\sigma}_i + e^{-i\omega_f t}\hat{\sigma}_i^\dagger)], \tag{1}$$

where $\hat{a}^\dagger(\hat{a})$ is the creation (annihilation) operator of the cavity field mode, $\hat{\sigma}_i^\dagger = |e\rangle_i\langle g|$ $(\hat{\sigma}_i = |g\rangle_i\langle e|)$ the raising (lowering) operator for the atomic transition at frequency ω_a, $\hat{\sigma}_{z,i} = |e\rangle_i\langle e| - |g\rangle_i\langle g|$, g the coupling constant of the atoms with the cavity field, Ω the Rabi frequency associated with the amplitude of the coherent field that drives the atoms. We can change to the interaction picture [31] by the unitary operator $\exp\{\frac{i}{\hbar}\hat{H}_0 t\}$ so that the system Hamiltonian (1) becomes $\hat{H}_i = \hat{H}_0' + \hat{H}_1'$ where:

$$\hat{H}_0' = \hbar(\Delta - \delta)\hat{a}^\dagger\hat{a} + \hbar\Delta\sum_{i=1}^{2}|e\rangle_i\langle e| + \hbar\Omega\sum_{i=1}^{2}\hat{\sigma}_{x,i}$$

$$\hat{H}_1' = \hbar g\sum_{i=1}^{2}(\hat{a}\hat{\sigma}_i^\dagger + \hat{a}^\dagger\hat{\sigma}_i). \tag{2}$$

We introduced the operators $\hat{\sigma}_{x,i} = \hat{\sigma}_i^\dagger + \hat{\sigma}_i$ $(i = 1, 2)$ and the detuning parameters $\delta = \omega_a - \omega_c$ and $\Delta = \omega_a - \omega_f$ for the atom-cavity mode and the atom-driving field, respectively.

We can also include the dissipative dynamics for the cavity mode at rate κ, when it is in contact with the environment, and the atomic decays at rate γ. Therefore, we describe the open system dynamics by the following master equation (ME) for the whole system statistical operator $\rho(t)$:

$$\dot{\rho} = -\frac{i}{\hbar}[\hat{\mathcal{H}}_i, \rho] + \hat{\mathcal{L}}_c\rho + \hat{\mathcal{L}}_a\rho, \tag{3}$$

where the square bracket denotes a commutator, $\hat{\mathcal{L}}_c$ is the standard Liouville super-operator for a damped harmonic oscillator at zero temperature

$$\hat{\mathcal{L}}_c\rho = -\frac{\kappa}{2}(\hat{a}^\dagger\hat{a}\rho - 2\hat{a}\rho\hat{a}^\dagger + \rho\hat{a}^\dagger\hat{a}) \tag{4}$$

and $\hat{\mathcal{L}}_a$ the standard Liouville super-operator for the decay of the atomic levels $|e\rangle_i$:

$$\hat{\mathcal{L}}_a\rho = -\frac{\gamma}{2}\sum_{i=1}^{2}(\hat{\sigma}_i^\dagger\hat{\sigma}_i\rho - 2\hat{\sigma}_i\rho\hat{\sigma}_i^\dagger + \rho\hat{\sigma}_i^\dagger\hat{\sigma}_i). \tag{5}$$

To identify the collapse and the "free evolution" operators for the MCWF method we rewrite the ME (3) in the Lindblad form:

$$\dot{\rho} = -\frac{i}{\hbar}(\hat{\mathcal{H}}_e\rho - \rho\hat{\mathcal{H}}_e^\dagger) + \sum_{i=1}^{3}\hat{C}_i\rho\hat{C}_i^\dagger \tag{6}$$

where the non-Hermitian effective Hamiltonian $\hat{\mathcal{H}}_e$ is

$$\hat{\mathcal{H}}_e = \frac{\hat{\mathcal{H}}_i}{g} - \frac{i\hbar}{2}\sum_{i=1}^{3}\hat{C}_i^\dagger\hat{C}_i, \tag{7}$$

and the collapse operators are $\hat{C}_{1,2} = \sqrt{\tilde{\gamma}}\hat{\sigma}_{1,2}$, $\hat{C}_3 = \sqrt{\tilde{k}}\hat{a}$. We have introduced the dimensionless time $\tilde{t} = gt$ so that the relevant dimensionless system parameters are:

$$\tilde{\Delta} = \frac{\Delta}{g}, \quad \tilde{\delta} = \frac{\delta}{g}, \quad \tilde{\Omega} = \frac{\Omega}{g}, \quad \tilde{\kappa} = \frac{\kappa}{g}, \quad \tilde{\gamma} = \frac{\gamma}{g}. \tag{8}$$

The system dynamics can be simulated by a suitable number N_{tr} of trajectories, i.e. stochastic evolutions of the

whole system wave function $|\psi_j(\tilde{t})\rangle$ $(j = 1, 2, ...N_{tr})$, by means of the following main rule

$$|\psi_j(\tilde{t}+\delta\tilde{t})\rangle = \begin{cases} \frac{(1-\frac{i}{\hbar}\hat{\mathcal{H}}_e\delta\tilde{t})|\psi_j(\tilde{t})\rangle}{\sqrt{1-\delta_p(\tilde{t})}} & \text{if } \delta_p(\tilde{t}) < N_{rnd} \\ \frac{\hat{C}_i|\psi_j(\tilde{t})\rangle}{\sqrt{\delta_p(\tilde{t})}} & \text{if } \delta_p(\tilde{t}) > N_{rnd} \end{cases}, \tag{9}$$

where $\delta\tilde{t}$ is a suitable small time interval, $\delta_p(\tilde{t})$ is the collapse probability at time $\tilde{t}$, and N_{rnd} is a random number generated from a uniform distribution in $[0, 1]$. We note that the collapse probability depends on the cavity field mean photon number $\langle\hat{N}\rangle(\tilde{t})$ and the excited state populations $p_{e,i}(\tilde{t})$, and can be evaluated as $\delta_p(\tilde{t}) = \delta\tilde{t}[\tilde{\kappa}\langle\hat{N}\rangle(\tilde{t}) + \tilde{\gamma}(p_{e,1}(\tilde{t}) + p_{e,2}(\tilde{t}))]$. Therefore, the statistical operator of the whole system can be approximated by averaging over the N_{tr} trajectories, i.e., $\rho(\tilde{t}) \cong \frac{1}{N_{tr}}\sum_{i=j}^{N_{tr}} |\psi_j(\tilde{t})\rangle\langle\psi_j(\tilde{t})|$. In the numerical results presented in the next sections we typically consider $N_{tr} = 500$, corresponding to reasonable computation times.

For the initial state of the tripartite system we consider a fully separable state where each atom is prepared in the ground or excited state and the cavity field is in the vacuum state $|0\rangle_F$. For example, if both atoms are in the ground state we have $|\psi(0)\rangle = |g\rangle_1 \otimes |g\rangle_2 \otimes |0\rangle_F \equiv |gg0\rangle$. The properties of the atom-atom subsystem are described by the reduced density operator obtained by a partial trace over the field variables $\rho_a(\tilde{t}) = \mathrm{Tr}_F\rho(\tilde{t})$. Likewise the properties of the two (equal) atom-field subsystems are described by the reduced density operator (e.g.) $\rho_{1F}(\tilde{t}) = \mathrm{Tr}_2\rho(\tilde{t})$ where the partial trace is taken over the variables of atom 2. To evaluate the degree of mixedness of the subsystem states we will consider the purities, e.g. $\mu_{12} = \mathrm{Tr}_a\rho_a^2$ for the atom pair. We choose to quantify the atom-atom entanglement by means of the entanglement of formation $\epsilon_F(\tilde{t})$ [32]. We shall compare the atom-atom and the atom-field entanglement in the case that only the Fock states $|0\rangle_F$ and $|1\rangle_F$ are relevant, so that the CV field mode can be approximated to a third qubit [13]. In that case we can consider the negativity $N_e = \max\{0, -\lambda^-\}$, where λ^- is the only one negative eigenvalue of the Partial Transpose [33] of the subsystem density matrix.

3 System dynamics in the strong coupling regime

In this section we consider the system dynamics under strong coupling conditions $g \gg \kappa, \gamma$, that are typical in CQED experiments in the case of atoms flying through a microwave cavity [9] and are also available for atoms stored inside high-finesse cavities [34]. We are mainly interested in the possibility to generate entangled states for the atom-atom subsystem and to investigate the entanglement sharing between subsystems. We first consider the resonant case under different driving conditions and then we focus on the detuned regimes.

3.1 Driving effect at resonance

Under resonant atom-driving field interaction ($\tilde{\Delta} = 0$), we can rewrite the Hamiltonian $\hat{H}_i$ in (2) by the unitary transformation $\exp(\frac{i}{\hbar}\hat{H}_0't)$ in the form:

$$\hat{H}_i'(t) = \hbar\frac{g}{2}\sum_{i=1}^{2}\{e^{-i\delta t}\hat{a}^\dagger[(1-e^{2i\Omega t})\hat{\sigma}_i^\dagger + (1+e^{2i\Omega t})\hat{\sigma}_i] + h.c.\}. \tag{10}$$

In addition, if we also consider atom-cavity mode resonant coupling ($\delta = 0$) and the strong driving limit ($\Omega \gg g$), the fast oscillating terms in (10) can be neglected leaving an effective Hamiltonian

$$\hat{H}_i'^{SD} = \hbar\frac{g}{2}\sum_{i=1}^{2}(\hat{a}+\hat{a}^\dagger)\hat{\sigma}_{x,i}. \tag{11}$$

The above equation outlines the simultaneous occurrence of the Jaynes-Cummings and the "anti-JC" interaction of each coherently driven atom with the cavity field [22–25]. In the limit of negligible atomic decays ($\gamma = 0$), the ME of the whole system can be solved exactly, even in the presence of cavity dissipation [35]. In this regime the absence in (11) of the driving field, whose action has been averaged, makes each atom independently interact with the cavity field. This implies the onset of interesting atom-atom correlations [22,24], also related to the decoherence of mesoscopic cavity field superposition states [36], but these correlations are classical [37]. This agrees with the result [37] that a single strongly driven atom in state $|g\rangle$ (or in $|e\rangle$) and a resonant cavity field mode in the vacuum state (or in any coherent state) can become maximally and permanently entangled within short times $\tilde{t} \sim 2$, that is a larger and more robust entanglement than in the standard JC system [38]. We remark that the effective Hamiltonian (11), in the case of only one atom, can also describe a more complex system in CQED composed by a three-level atom in Λ-configuration interacting with an optical cavity and driven by suitably detuned laser fields; the system realizes a Strongly-Driven One-Atom Laser [39].

If we do not consider the above strong driving limit we find that entangled atomic states can be generated up to $\tilde{\Omega} \simeq 5$. However the atomic entanglement of formation is irregular in time and rather weak.

3.2 Off-resonance dynamics: generation of maximally entangled atomic states

3.2.1 Moderated detuning regime

Under strong coupling conditions, dimensionless detuning $\tilde{\delta} = O(1)$, and for weak driving field amplitude $\tilde{\Omega} \approx \tilde{\delta}$, we find evidence of atom-atom entanglement, but the entanglement of formation ϵ_F remains rather low and is quite irregular in time, as the whole system dynamics. In the

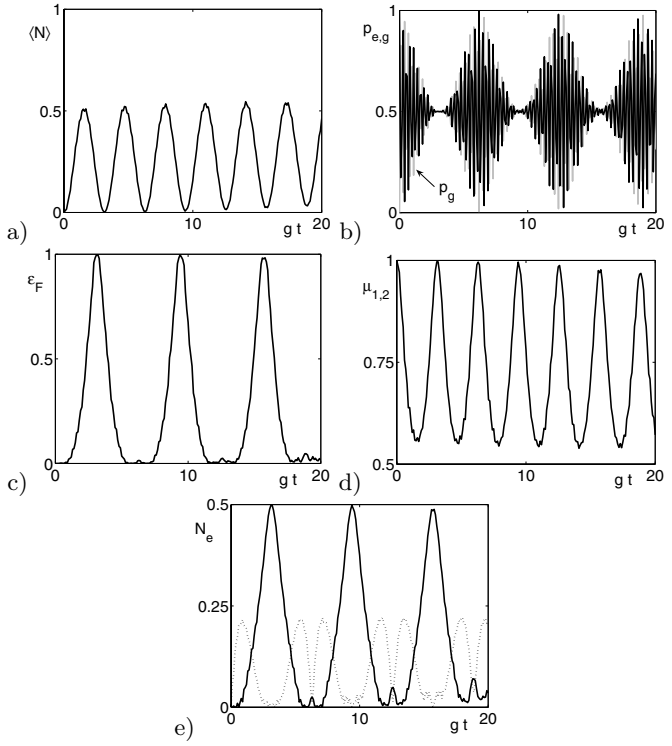

Fig. 1. System dynamics in the strong coupling regime ($\tilde{\kappa} = 10^{-3}$, $\tilde{\gamma} = 10^{-4}$) for $\tilde{\Delta} = 0$, $\tilde{\delta} = 2$, and $\tilde{\Omega} = 20$: (a) cavity mean photon number, (b) atomic populations, (c) atom-atom entanglement of formation, (d) purity of the atom-atom states, (e) negativity of the atom-atom (solid line) and atom-cavity field (dotted line) states.

rest of this subsection we shall concentrate on the much more interesting case of the strong driving regime, $\tilde{\Omega} \gg \tilde{\delta}$.

Let us start with the case $\tilde{\delta} = 2$, $\tilde{\Omega} = 20$, where the detuning value $\delta = 2g$ corresponds to the vacuum Rabi frequency. Figures 1a–1e show that the system exhibits a periodical behavior. The cavity field mean photon number $\langle \hat{N} \rangle$ (Fig. 1a) oscillates between zero and roughly 0.5 at the detuning frequency. The atomic populations $p_{e,g}$ (Fig. 1b), that are equal for both atoms, exhibit a repeated collapse-and-revival evolution with a doubled period, modulating the fast driven oscillations. Most important (Fig. 1c) the atom-atom entanglement of formation ϵ_F shows the generation of maximally entangled states at times $gt_k = (2k+1)\pi$, $(k = 0, 1, ...)$, whereas quantum correlations are negligible in between. All these peaks coincide with vanishing values of the mean photon number and with collapsed atomic populations, corresponding to the single atoms in maximally mixed states. In Figure 1d the atomic purity μ_{12} exhibits maxima thus demonstrating that at times gt_k the tripartite system is in a bi-separable state, where the atoms turn out to be in superpositions of Bell states and the cavity field is in the vacuum state:

$$|\phi_B(t_k)\rangle = \frac{|\Phi^+\rangle \mp i|\Phi^-\rangle}{\sqrt{2}} \otimes |0\rangle_F \propto \frac{|gg\rangle \mp i|ee\rangle}{\sqrt{2}} \otimes |0\rangle_F \tag{12}$$

where the upper (lower) sign refers to the time $gt_0 = \pi$ ($gt_1 = 3\pi$) of the first (second) maximum of atomic quantum correlations. The same result is obtained starting with both atoms in the excited state. In the case of atoms prepared in different states, we find the same superpositions of the other two Bell states, i.e.:

$$|\psi_B(t_k)\rangle = \frac{|\Psi^+\rangle \mp i|\Psi^-\rangle}{\sqrt{2}} \otimes |0\rangle_F \propto \frac{|ge\rangle \mp i|eg\rangle}{\sqrt{2}} \otimes |0\rangle_F. \tag{13}$$

Figure 1d also shows that the atomic purity, like the mean photon number, actually peaks at twice the frequency of the atomic entanglement of formation, that is negligible in between the main ones. On the other hand the atomic populations of Figure 1b show simultaneous maxima of the lower state population p_g. Hence we can argue that at these dimensionless times, $gt_k = 2k\pi$ $(k = 1, 2, ...)$, the system is very close to a pure and fully separable state that is in fact the initial state $|g\rangle_1 \otimes |g\rangle_2 \otimes |0\rangle_F$. This holds also for the other atomic initial states. These results generalize the prediction of pure separable cavity field-single atom states for certain interaction times in the standard (undriven) JC system [40]. The global picture is fully confirmed in Figure 1e where we compare the atom-atom and the atom-field negativities. This case nicely shows the generation and the dynamical distribution of system entanglement, which periodically concentrates on the bipartite subsystems as well as nearly vanishes when the system closely approaches the initial fully separable state.

We remark that the transformation $|gg\rangle \mapsto \frac{1}{\sqrt{2}}(|gg\rangle - i|ee\rangle)$ for the atomic part of (12) was proposed in [41] to implement, together with single-ion operations, the C-NOT gate with two trapped ions. Furthermore, let us consider the transformations (12) and (13) at time $gt_0 = 3\pi$ for atoms prepared in states $|gg\rangle$, $|ge\rangle$ and $gt_1 = \pi$ for atoms initially in $|ee\rangle$, $|eg\rangle$, i.e.

$$\begin{aligned} |gg\rangle, |ee\rangle &\mapsto \frac{|gg\rangle \pm i|ee\rangle}{\sqrt{2}} \\ |ge\rangle, |eg\rangle &\mapsto \frac{|ge\rangle \pm i|eg\rangle}{\sqrt{2}} \end{aligned} \tag{14}$$

where the first (second) state transforms with the upper (lower) sign. Relations (14) provide a logic gate that was implemented for two trapped ions [30] and, together with single-qubit rotations, can realize universal quantum logic [23].

In Figure 2 we consider the case $\tilde{\delta} = 2$, $\tilde{\Omega} = 200$, i.e., a driving field amplitude larger than in the previous case by one order of magnitude. The global picture now shows only partial elements of periodicity. The mean photon number, reported in Figure 2a, still oscillates at the detuning frequency, with higher peaks than in Figure 2a. On the contrary (Fig. 2b) the atomic populations collapse and after a tiny revival remain at the stationary value of 0.5. In Figures 2c and 2d we see that maximally pure entangled atomic states are generated at the same times, $gt'_k = k\pi$, $(k = 1, 2, ...)$, as the zeros of the mean photon

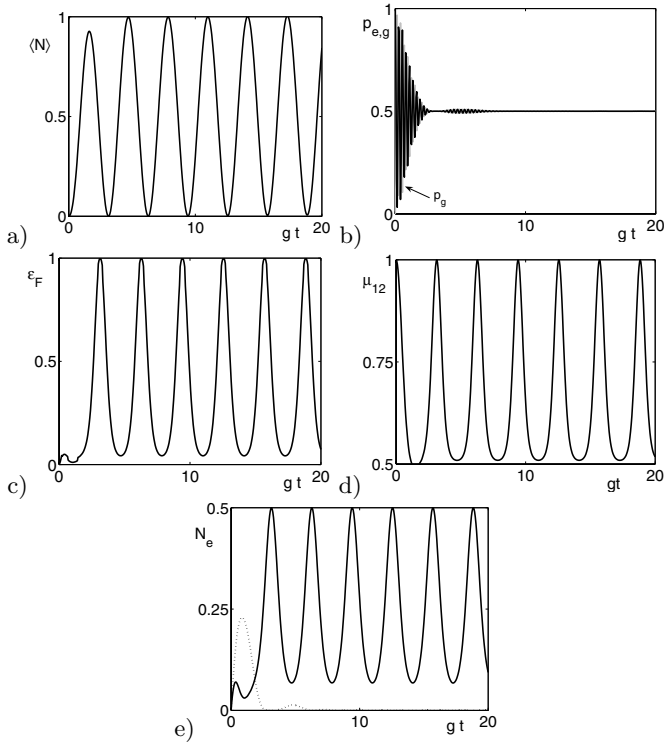

Fig. 2. System dynamics in the strong coupling regime ($\tilde{\kappa} = 10^{-3}$, $\tilde{\gamma} = 10^{-4}$) for $\tilde{\Delta} = 0, \tilde{\delta} = 2, \tilde{\Omega} = 200$: (a) cavity mean photon number, (b) atomic populations, (c) atom-atom entanglement of formation, (d) purity of the atom-atom states, (e) negativity of the atom-atom (solid) and atom-cavity field (dotted) states.

number, i.e., at a doubled frequency than in Figure 1c. Hence the robust increase in the driving field amplitude prevents the system from returning very close to the initial completely uncorrelated state. The bi-separable states at times t'_k consist in Bell states for the atom pair correlated with the cavity field vacuum state:

$$|g,g,0\rangle, |e,e,0\rangle \mapsto \frac{|gg\rangle + |ee\rangle}{\sqrt{2}} \otimes |0\rangle_F = |\Phi^+\rangle \otimes |0\rangle_F,$$
$$|g,e,0\rangle, |e,g,0\rangle \mapsto \frac{|ge\rangle + |eg\rangle}{\sqrt{2}} \otimes |0\rangle_F = |\Psi^+\rangle \otimes |0\rangle_F. \tag{15}$$

Furthermore, the behavior of the bipartite subsystem negativities in Figure 2e shows that the atoms and the cavity field become partially quantum correlated only at the early stage of system dynamics. The latter result has however only a qualitative value because the approximation of the cavity field as a qubit is very rough in this case.

3.2.2 Dispersive regime

Now we consider the large detuning limit of atom-cavity field coupling, $\tilde{\delta} \gg 1$. We note that the JC Hamiltonian

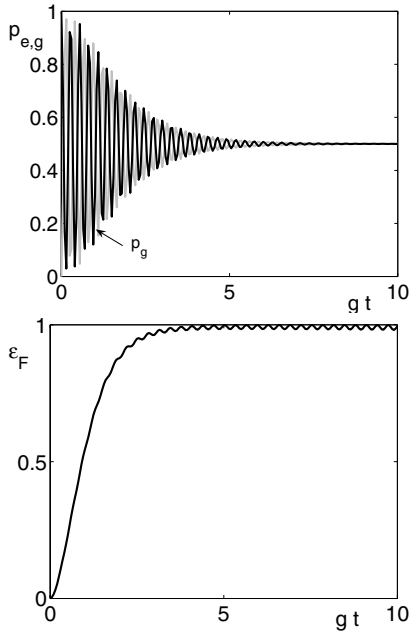

Fig. 3. System dynamics in the strong coupling regime ($\tilde{\kappa} = 10^{-3}$, $\tilde{\gamma} = 10^{-4}$) for $\tilde{\Delta} = 0$, $\tilde{\delta} = 20$, $\tilde{\Omega} = 200$: (a) atomic populations, (b) atom-atom entanglement of formation ϵ_F.

$\hat{H}'_1$ of (2) could be replaced by an effective Hamiltonian [9]

$$\hat{H}_1^D = \hbar \frac{g^2}{\delta} \sum_{i=1}^{2} (\hat{\sigma}_i^\dagger \hat{\sigma}_i + \hat{a}^\dagger \hat{a} \hat{\sigma}_{z,i}) \tag{16}$$

that describes a purely dispersive regime where there is no energy exchange between the atoms and the cavity field, and the coupling constant is reduced to g^2/δ. Note that atom-atom entanglement without driving field was demonstrated [14] due to the occurrence of dipole-dipole coupling for atoms prepared in different states [42]. By applying to (16) the same unitary transformation $\exp(\frac{i}{\hbar}\hat{H}'_0 t)$ as to (2) we would obtain, instead of (10), the Hamiltonian

$$\hat{H}_i'^D(t) = \hbar \frac{g^2}{2\delta} \sum_{i=1}^{2} [\hat{1}_i - (1 + 2\hat{a}^\dagger \hat{a})(e^{2i\Omega t}\hat{\sigma}_i^\dagger + e^{-2i\Omega t}\hat{\sigma}_i)]. \tag{17}$$

Hence also in this regime we can well expect the generation of atomic entanglement because the previously discussed physical mechanism is still present, though there is no direct coupling between atomic polarizations. Furthermore, we expect that the atomic entanglement is by no means limited by the occurrence of atom-field entanglement, because the field remains nearly decoupled from system dynamics.

Also in the dispersive regime, like in the case of moderate detuning, the strong driving limit $\tilde{\Omega} \gg 1$ leads to the most interesting results. In Figure 3 we show numerical results in the case $\tilde{\delta} = 20$, $\tilde{\Omega} = 200$. As expected, the cavity field always remains close to the initial vacuum state due to the strong detuning with the atoms. Figure 3a shows a

collapse of atomic populations, without trace of revival on the time scale of interest for physical implementations. By the time that the single atoms have decohered into a maximally mixed state, the atomic entanglement of formation has reached the maximum value, where it remains with negligible oscillations (Fig. 3b). Actually there is no competition with negligible atom-field entanglement. Hence we find the fast generation of nearly stationary atomic Bell states, in particular: $|g,g,0\rangle$,$|e,e,0\rangle \mapsto |\Phi^+\rangle \otimes |0\rangle_F$ and $|g,e,0\rangle$,$|e,g,0\rangle \mapsto |\Psi^+\rangle \otimes |0\rangle_F$. The tiny oscillations correspond to states very close (in all cases) to superpositions of the atomic Bell states $|\Phi^+\rangle$ and $|\Psi^+\rangle$.

For driving field amplitude $\Omega \ll \delta$ the system dynamics is almost periodic, as well as the atomic entanglement that can be maximum but only after time intervals rather long for realistic implementations. For $\Omega \simeq \delta$ the dynamics becomes faster: e.g., in the case $\tilde{\Omega} = \tilde{\delta} = 10$ the first peak with $\epsilon_F(\tilde{t}) = 1$ occurs at $\tilde{t} \simeq 10$. The periodicity is lost and the build-up of atomic entanglement evolves towards the fast and monotonic growth to the maximum value as described in the strong driving regime.

4 The effect of dissipation

In this section we consider the effect of dissipation, in case that the strong coupling conditions between the atoms and the cavity field cannot be implemented.

First we investigate the regime of moderate detuning and strong atomic driving as in Figures 1 and 2. In this regime we focus on the effect of cavity dissipation, assuming that the decay of atomic levels is negligible during the interaction, as is usually the case in the microwave domain [9], and may be the case for effective two-level systems in the optical domain [22]. In Figure 4 we show numerical results for the mean photon number, the atomic entanglement of formation, and the atomic purity, with the same parameters as in Figure 1 and for three values of the dimensionless cavity decay rate, from $\tilde{k} = 0.01$ to $\tilde{k} = 0.5$. For $\tilde{k} = 0.01$ we see that the system dynamics is unaffected by dissipation so that the periodic generation of superpositions of atomic Bell states predicted in the strong coupling regime remains valid. At the other extreme, for $\tilde{k} = 0.5$, the system approaches a steady-state via damped oscillations with vanishing atomic entanglement, while the atomic purity is heavily degraded. In Figure 5 we show numerical results with the same parameters as in Figure 2 for the same quantities and the same dimensionless cavity decay rate values as in Figure 4. For $\tilde{k} = 0.01$ we see again that the system dynamics is not affected by cavity dissipation so that the prediction of periodic generation of atomic Bell states under strong coupling conditions is confirmed. On the contrary, for $\tilde{k} = 0.5$ the system reaches a steady-state, where the atomic entanglement vanishes and the atoms are in a maximally mixed sum of the two relevant Bell states, i.e., $\frac{1}{2}(|\Phi^+\rangle\langle\Phi^+| + |\Psi^+\rangle\langle\Psi^+|)$. In Figures 4 and 5 we fixed a dimensionless atomic decay rate $\tilde{\gamma} = 10^{-4}$, but the results remain almost identical up to $\tilde{\gamma} = 10^{-3}$.

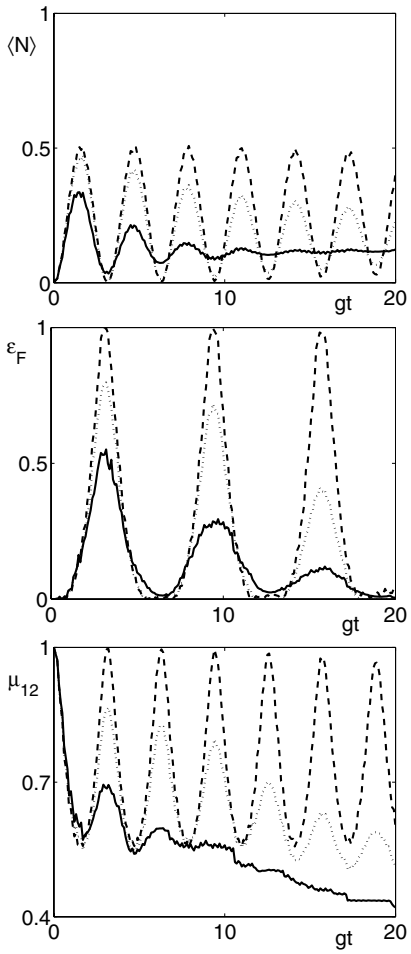

Fig. 4. Dissipative regime under moderate detuning ($\tilde{\delta} = 2$) and strong driving conditions ($\tilde{\Omega} = 20$), with negligible atomic decay rate ($\tilde{\gamma} = 10^{-4}$): (a) cavity field mean photon number $\langle \hat{N} \rangle$, (b) atom-atom entanglement of formation ϵ_F, (c) atom-atom purity μ_{12}. Dimensionless decay rate $\tilde{k} = 0.01$ (dashed), 0.1 (dotted), 0.5 (solid).

On the other hand, in the strong driving and dispersive coupling regime as in Figure 3, where nearly stationary Bell states can be generated, cavity dissipation does not affect the atomic quantum correlations at all, since the cavity field always remains negligible. In this regime we consider the possible effect of atomic decay. Hence in Figure 6 we report the atomic entanglement of formation and purity with the parameter of Figure 3, dimensionless cavity decay rate $\tilde{k} = 0.5$, and dimensionless atomic decay rates ranging from $\tilde{\gamma} = 0.001$ to $\tilde{\gamma} = 0.1$, showing how the increase of atomic dissipation might affect the generation of almost stationary Bell states predicted under strong coupling conditions.

5 Conclusions

We have described the dynamics and the quantum correlations of an open tripartite system in cavity QED, where

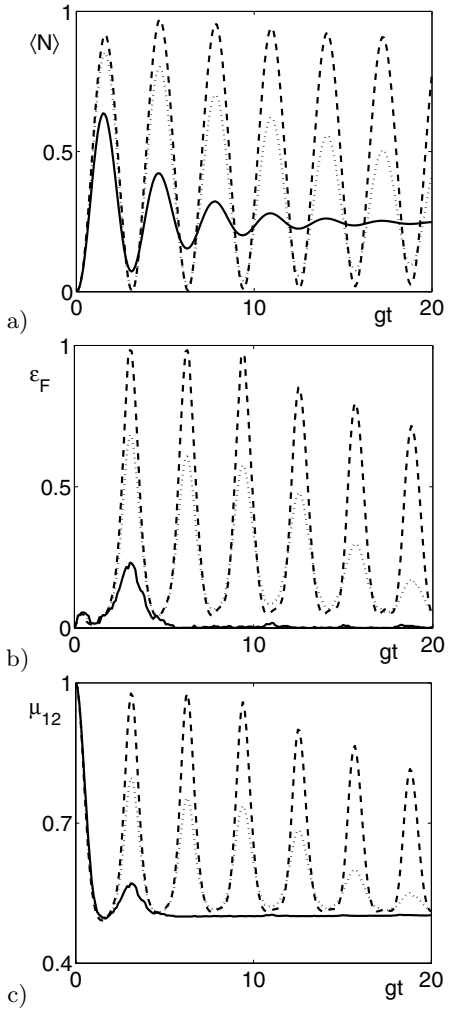

Fig. 5. Dissipative regime under moderate detuning ($\tilde{\delta} = 2$) and strong driving conditions ($\tilde{\Omega} = 200$), with negligible atomic decay rate ($\tilde{\gamma} = 10^{-4}$): (a) cavity field mean photon number $\langle \hat{N} \rangle$, (b) atom-atom entanglement of formation ϵ_F, (c) atom-atom purity μ_{12}. Dimensionless decay rate $\tilde{k} = 0.01$ (dashed), 0.1 (dotted), 0.5 (solid).

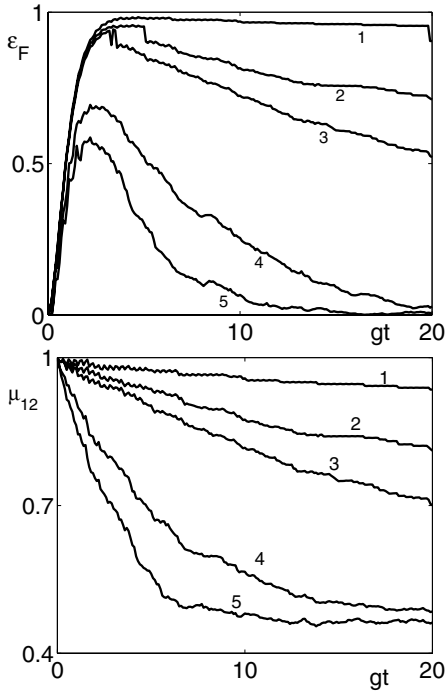

Fig. 6. Dissipative regime under dispersive coupling ($\tilde{\delta} = 20$) and strong driving conditions ($\tilde{\Omega} = 200$), with cavity decay rate ($\tilde{k} = 0.5$): (a) atom-atom entanglement of formation ϵ_F, (b) atom-atom purity μ_{12}. Dimensionless atomic decay rate $\tilde{\gamma} = 0.001$ (1), 0.005 (2), 0.01 (3), 0.05 (4), 0.1 (5).

two coherently driven two-level atoms interact with a cavity mode that is weakly coupled to the environment. This system can be implemented with current or forthcoming state of the art in the microwave or optical domains.

We have found two interesting regimes for the generation of maximally entangled atomic states. The first one is a regime of moderate detuning under strong driving conditions: $\tilde{\Omega} \gg \tilde{\delta} \sim 1$. Atomic Bell states can be generated at given interaction times and for low enough values of the cavity decay rate. Bell states superpositions are also available for logic gates proposed and demonstrated with trapped ions [23,30]. Bi-separable and fully separable states can be generated. Also we describe how the quantum correlations oscillate between the different subsystems. The second interesting regime is obtained for purely dispersive atom-field coupling combined with strong atomic driving: $\tilde{\Omega} \gg \tilde{\delta} \gg 1$. Here the cavity field always remains quite close to the initial vacuum state and only acts as a catalyst for the formation of entangled atomic states, as in the experiment of [14]. This allows the generation of nearly stationary atomic Bell states, that are not affected by cavity dissipation.

In both regimes the underlying physical mechanism is that the atoms are driven by the same coherent field while off-resonantly undergo JC and anti-JC interactions with the cavity field. Under reasonable control of the coupling constants and the interaction times this mechanism appears to be scalable for applications in quantum information processing and computation. In the strong driving limit but for resonant atom-field interaction the above mechanism is instead inhibited because the atoms become fully quantum-correlated with the cavity field [37].

The results presented in this paper extend and basically complete the general picture on the entanglement properties of this system in all main dynamical regimes.

This work has been supported by MIUR through the project PRIN-2005024254-002.

References

1. J.A. Wheeler, W.H. Zurek, *Quantum Theory and Measurement* (Princeton University Press, Princeton 1983)
2. J.S. Bell, Physics (NY) **1**, 195 (1964)
3. A. Aspect, Nature **398**, 189 (1999)
4. M. Genovese, Phys. Rep. **413**, 319 (2005)

5. M.A. Nielsen, I.L. Chuang, *Quantum Computation and Quantum Information* (Cambridge University Press, Cambridge 2000)
6. V. Coffman, J. Kundu, W.K. Wootters, Phys. Rev. A **61**, 052306 (2000); G. Jaeger, *Quantum Information An Overview* (Springer, New York 2007)
7. M. Paternostro et al., Phys. Rev. B **69**, 214502 (2004); J. Zou et al., Phys. Rev. A **73**, 042319 (2006); J. Lee et al., Phys. Rev. Lett. **96**, 080501 (2006); F. Casagrande, A. Lulli, M.G.A. Paris, Phys. Rev. A **75**, 032336 (2007)
8. P. Zoller, Eur. Phys. J. D **36**, 203 (2005)
9. S. Haroche, J.M. Raimond, *Exploring the Quantum* (Oxford University Press, Oxford 2006)
10. H. Walther et al., Rep. Prog. Phys. **69**, 1325 (2006)
11. H. Mabuchi, A.C. Doherty, Science **298**, 1372 (2002); C. Monroe, Nature **416**, 238 (2002)
12. J.A. Sauer et al., Phys. Rev. A **69**, 051804(R) (2004)
13. F. Hagley et al., Phys. Rev. Lett. **79**, 1 (1997)
14. S. Osnaghi et al., Phys. Rev. Lett. **87**, 037902 (2001)
15. W. Tittel, G. Weihs, Quant. Inf. Comput. **2**, 3 (2001)
16. J. Volz et al., Phys. Rev. Lett. **96**, 030404 (2006)
17. Q. Zhang et al., Nature Phys. **2**, 678 (2006)
18. J.F. Sherson et al., Nature **443**, 557 (2006)
19. D. Leibfried et al., Rev. Mod. Phys. **75**, 281 (2003); D. Leibfried et al., Nature **438**, 639 (2005); H. Häffner et al., Nature **438**, 643 (2005)
20. E.T. Jaynes, F.W. Cummings, Proc. IEEE **51**, 89 (1963)
21. P. Alsing, D.S. Guo, H.J. Carmichael, Phys. Rev. A **45**, 5135 (1992)
22. E. Solano, G.S. Agarwal, H. Walther, Phys. Rev. Lett. **90**, 027903 (2003)
23. A. Sørensen, K. Molmer, Phys. Rev. Lett. **82**, 1971 (1999)
24. P. Lougovski et al., Phys. Rev. A **69**, 023812 (2004); F. Casagrande et al., Opt. Spectrosc. **99**, 301 (2005)
25. G.P. Guo et al., Phys. Rev. A **65**, 042102 (2002); S.B. Zheng, Phys. Rev. A **66**, 060303(R) (2002); L. Ye et al., Phys. Rev. A **72**, 034304 (2005); B.M. Rodriguez-Lara, H. Moja-Cessa, A.B. Klimov, Phys. Rev. A **71**, 023811 (2005); S.B. Zheng, Phys. Rev. A **74**, 043803 (2006); C.Y. Chen et al., Phys. Rev. A **73**, 032344 (2006); Z.Y. Xue, Y.M. Yi, Z.L. Cao, Physica A **374**, 119 (2007)
26. J. Dalibard, Y. Castin, K. Mølmer, Phys. Rev. Lett. **68**, 580 (1992)
27. E. Jane, M.B. Plenio, D. Jonathan, Phys. Rev. A **65**, 050302(R) (2002)
28. J. McKeever et al., Nature **425**, 268 (2003); S. Nussmann et al., Nature Phys. **1**, 122 (2005)
29. J. Eschner et al., Fortschr. Phys. **51**, 359 (2003); M. Keller et al., Appl. Phys. B **76**, 125 (2003)
30. D. Kielpinski et al., Science **291**, 1013 (2001)
31. S.M. Barnett, P.M. Radmore, *Methods in Theoretical Quantum Optics* (Clarendon Press, Oxford 1997)
32. S. Hill, W.K. Wootters, Phys. Rev. Lett. **78**, 5022 (1997)
33. A. Peres, Phys. Rev. Lett. **77**, 1413 (1996); M. Horodecki, P. Horodecki, R.P. Horodecki, Phys. Lett. A **223**, 1 (1996)
34. J. Ye, D.W. Vernooy, H.J. Kimble, Phys. Rev. Lett. **83**, 4987 (1999); P.W.H. Pinkse et al., Nature **404**, 365 (2000)
35. M. Bina, F. Casagrande, A. Lulli, in preparation
36. F. Casagrande, A. Lulli, Eur. Phys. J. D **36**, 123 (2005); F. Casagrande, A. Lulli, J. Opt. B: Quantum Semicl. Opt. **7**, S437 (2005)
37. F. Casagrande, A. Lulli, Int. J. Mod. Phys. B **20**, 1613 (2006); F. Casagrande, A. Lull, Int. J. Quant. Inf. **5**, 143 (2007)
38. C.C. Gerry, P.L. Knight, *Introductory Quantum Optics* (Cambridge University Press, Cambridge, 2005)
39. P. Lougovski et al., Phys. Rev. A **76**, 033802 (2007)
40. J. Gea-Banacloche, Phys. Rev. Lett. **65**, 3385 (1990)
41. A. Sorensen, K. Molmer, Phys. Rev. Lett. **62**, 022311 (2000)
42. S.B. Zheng, G.C. Guo, Phys. Rev. Lett. **85**, 022311 (2000)